

Differential effects of ciguatoxin and maitotoxin in primary cultures of cortical neurons

Victor Martin¹, Carmen Vale^{1*}, Alvaro Antelo², Masahiro Hiram³, Shuji Yamashita³, Mercedes R. Vieytes⁴, Luis M. Botana^{1*}

¹Departamento de Farmacología, Facultad de Veterinaria, Universidad de Santiago de Compostela, Campus Universitario s/n, 27002, Lugo

²Laboratorios Cifga, Facultad de Veterinaria, Universidad de Santiago de Compostela, Campus Universitario s/n, 27002, Lugo

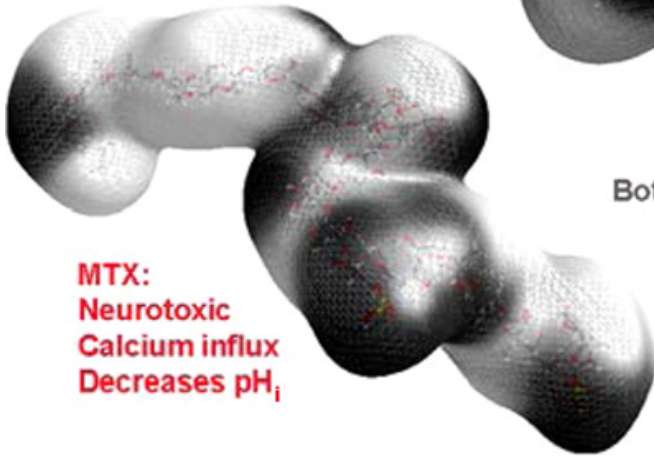
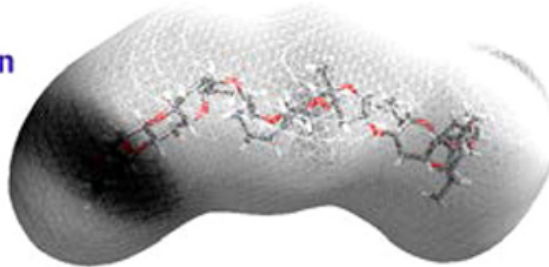
³Department of Chemistry, Graduate School of Science, Tohoku University, Sendai 980-8578, Japan.

⁴ Departamento de Fisiología, Facultad de Veterinaria, Universidad de Santiago de Compostela, Campus Universitario s/n, 27002, Lugo

KEYWORDS. Ciguatoxin, CTX 3C, maitotoxin, voltage-gated channel, cortical neuron, cytosolic calcium concentration, intracellular pH, neurotoxicity.

Table of Contents Graphic

**CTX 3C: hiperpolarizing shift
in VGSC activation & inactivation**



**MTX:
Neurotoxic
Calcium influx
Decreases pH_i**

**Both: No effect on VGCC and K_V
Block peak I_{Na}**

Abstract

Ciguatoxins (CTXs) and maitotoxins (MTXs) are polyether ladder shaped toxins derived from the dinoflagellate *Gambierdiscus toxicus*. Despite MTXs are 3 times larger than CTXs, part of the structure of MTX resembles that of CTX. To date, the synthetic ciguatoxin, CTX 3C has been reported to activate voltage gated sodium channels whereas the main effect of MTX is inducing calcium influx into the cell leading to cell death. However there is a lack of information regarding the effects of these toxins in a common cellular model. Here, in order to have an overview of the main effects of these toxins in mice cortical neurons, we examined the effects of MTX and the synthetic ciguatoxin CTX 3C on the main voltage dependent ion channels in neurons, sodium, potassium and calcium channels as well as on membrane potential, cytosolic calcium concentration $[Ca^{2+}]_c$, and neuronal viability. Regarding voltage gated ion channels, neither CTX 3C nor MTX affected voltage gated calcium or potassium channels, but while CTX 3C had a large effect on voltage gated sodium channels (VGSC) by shifting the activation and inactivation curves to more hyperpolarized potentials and decreasing peak sodium channel amplitude, MTX, at 5 nM, had no effect on VGSC activation and inactivation but decreased peak sodium current amplitude. Other major differences between both toxins were the massive calcium influx and intracellular acidification produced by MTX but not by CTX 3C. Indeed, the novel finding that MTX produces acidosis supports a pathway recently described in which MTX produces calcium influx via the sodium hydrogen exchanger (NHX). For the first time, we found that VGSC blockers partially blocked the MTX-induced calcium influx, intracellular acidification and protected against the short term MTX-induced cytotoxicity. The results presented here, provide the first report that shows the comparative effects of two prototypical ciguatera toxins, CTX 3C and MTX, in a neuronal model. We hypothesize that the analogies and differences in the bioactivity of these two toxins, produced by the same microorganism, may be strongly linked to their chemical structure.

Introduction

Ciguatera, one of the most widespread and fearful form of seafood poisoning, is caused by the consumption of fish containing toxins produced by *Gambierdiscus toxicus*.¹ This marine dinoflagellate produces several bioactive polyether compounds such as MTXs, CTXs and gambierol.²⁻⁵ The most common symptoms of ciguatera, comprise gastrointestinal and cardiac disturbances as well as neurological alterations, such as intense pruritus, painful dysesthesias, allodynia, ataxia and hyperalgesia, among others.⁴ The synthetic ciguatoxin CTX 3C is a highly lipophilic cyclic polyether compound characterized by 13 ether rings.⁵ The structure of MTX is, in part, similar to that of CTXs, with many ether rings forming ladder shaped polyether compounds.⁶

The neurological symptoms of ciguatera food poisoning are believed to be the consequence of the direct interaction of CTX with voltage-gated sodium channels (VGSC) targeting the site 5 of their α -subunit.^{4,7} In neuronal cells, this interaction produces a shift in the voltage dependence of the channel activation to more negative potentials and inhibits VGSC inactivation, causing resting membrane depolarization by increasing Na^+ influx.⁸⁻¹⁰ Apart from that, it has been described that CTX promotes mobilization of intracellular Ca^{+2} dependent on Na^+ influx through VGSC in neuroblastoma x glioma hybrid cells and stimulates the inositol 1,4,5 triphosphate-releasable Ca^{+2} store.¹¹ At the neuromuscular junction, CTX produces transient neuronal discharges and trains of repetitive action potentials.¹²

MTX, one of the largest nonpolymeric natural products so far known,^{13, 14} is one of the most potent marine toxins known to date. It is a potent activator of Ca^{+2} influx in a wide variety of cells.¹⁵ However, there is a great controversy regarding the mechanism for MTX-induced calcium influx. It has been proposed that MTX causes opening of non-selective, non-voltage activated ion channels, which allows massive Ca^{+2} influx and leads to cellular toxicity.¹⁶ In neuroblastoma–glioma hybrid cells and certain pituitary tumor cells, MTX-elicited Ca^{+2} influx was blocked at least in part by dihydropyridines that are selective blockers of type L voltage-dependent Ca^{+2} channels.¹⁵ However, in other experimental models such as smooth muscle cells¹⁷ and synaptosomes,¹⁸ these Ca^{+2} channel antagonists had no effect on the MTX-elicited Ca^{+2} influx. Apart from these differences in MTX effects in several cellular models, there is a lack of information regarding the effects of MTX in voltage gated channels in neurons. It is noteworthy that VGSC have been reported to be involved in other phycotoxin-induced rise in

intracellular calcium, as described for palitoxin (PTX).¹⁹ In that case, intracellular calcium influx was strongly linked to pH disturbances leading to intracellular acidification.²⁰ Recently, it has been suggested that in rat cortical neurons, the sodium-hydrogen exchanger (NHX) plays a key role in the MTX induced calcium influx and neurotoxicity.²¹ It has also been suggested that by lowering extracellular pH, MTX-dependent calcium influx decreases.^{21, 22}

Since both, CTX 3C and MTX, are polyether compounds produced by the same microorganism and part of the chemical structure of MTX resembles that of CTX 3C, it is possible that they could share similar cellular effects. However, most of the information to date appears in the context of a wide range of different cellular models which makes really difficult to identify the cellular effects of each toxin in a common model. Our aim here was to compare the neurological actions of CTX 3C and MTX in neurons. Thus, we followed a parallel study of both toxins considering neuronal toxicity, intracellular calcium and pH, and effects on the main ion channels responsible for neuronal excitability and electrical signaling: voltage-gated calcium, sodium, and potassium channels in cortical neurons. Moreover, since a known effect of ciguatoxin is to depolarize the cell membrane, we studied the effect of MTX on membrane potential in the same experimental conditions.

Up to date, MTX has been classified into the group of neurotoxins acting on non-specific channels.²³ However, the results presented here indicate that MTX also affects neuronal VGSC. In contrast, neither CTX 3C nor MTX affected voltage gated calcium and potassium channels. Interestingly, CTX 3C shifted the activation and inactivation curves of VGSC to more hyperpolarized potentials but MTX had no effect on VGSC activation and inactivation. Maitotoxin, but not CTX 3C, increased intracellular calcium concentration and produced intracellular acidosis in neurons. Indeed, MTX but not CTX 3C was toxic to neurons in a concentration dependent manner. Here, we further demonstrate that the MTX-induced Ca^{+2} influx and intracellular acidification were ameliorated by voltage-gated sodium channel blockers. Furthermore, MTX depolarized the membrane potential and again, this effect was decreased by blockade of VGSC.

Although several reports have investigated the cellular effects of MTX and CTX 3C in several cell types, much information is controversial and can lead to confusion when comparing the effects of both toxins. The present work, using cultured cortical neurons, was designated to

compare the effects of the two compounds from *Gambierdiscus toxicus* in a common neuronal model.

Materials and Methods

Primary cultures of cortical neurons. Swiss mice were used to obtain primary cultures of cortical neurons. All protocols were approved by the University of Santiago de Compostela Institutional animal care and use committee. Primary cortical neurons were obtained from embryonic day 16–18 Swiss mice. Briefly, cerebral cortices were removed and dissociated by mild trypsinization, followed by mechanical trituration in a DNase solution (0.004% w/v) containing a soybean trypsin inhibitor (0.05% w/v). The cells were suspended in Neurobasal medium supplemented with 1% B-27 supplement (Invitrogen), 5 mM L-glutamine, and 1% penicillin/streptomycin. The cell suspension was seeded in 12 well plates precoated with poly-D-lysine and the cell culture was kept in a 95% air, 5% CO₂ atmosphere at 37 °C. Culture medium was replaced every 3-4 days. Neurons were employed between 5 and 12 days in culture.²⁴

Determination of cellular viability. Cell viability was assessed by the MTT (3-[4,5-dimethylthiazol-2-yl]-2,5-diphenyltetrazolium bromide) test, as previously described.²⁵ The assay was performed in cultures grown in 96 well plates and exposed to concentrations of maitotoxin ranging from 0.001 to 1 nM or CTX 3C from 0.01 to 10 nM, added to the culture medium. Cultures were maintained in the presence of the toxin at 37 °C in humidified 5% CO₂/95% air atmosphere for 24 hours (otherwise noted). Saponin was used as cellular death control and its absorbance was subtracted from the other data. After the exposure time, cells were rinsed and incubated for 60 min with a solution of MTT (500 µg ml⁻¹) dissolved in Locke's buffer containing in mM: 154 NaCl, 5.6 KCl, 1.3 CaCl₂, 1 MgCl₂, 10 HEPES and 5.6 glucose (pH 7.4). After washing off excess MTT, cells were disaggregated with 5% sodium dodecyl sulfate and the absorbance of the colored formazan salt was measured at 595 nm in a spectrophotometer plate reader.

Electrophysiology. Whole cell patch-clamp recordings, achieved by gentle mechanical suction of the membrane patch, were performed in cortical neurons between 5-12 days in culture (otherwise noted), at room temperature (22-25°C). Neurons with a bright and smooth appearance were selected for recording. A computer-controlled current and voltage clamp amplifier (Multiclamp 700B, Molecular Devices) was used. Signals were recorded and analyzed using a

Pentium computer equipped with a Digidata 1440 data acquisition system and pClamp10 software (Molecular Devices, Sunnyvale, CA). pClamp10 was used to generate current and voltage-clamp commands and to record the resulting data. Signals were filtered at 10 kHz and digitized at 20 μ s intervals. Series resistance was compensated by 80% when possible. After establishing the whole-cell configuration, neurons were allowed to stabilize for at least 5 min before current recording protocols were initiated to ensure adequate equilibration between the internal pipette solution and the cell interior. Recording electrodes were fabricated from borosilicate glass micro capillaries (outer diameter, 1.5 mm), and the tip resistance was 5-10 M Ω . Culture medium was exchanged with several washes of recording solution immediately prior to the experiment.

For voltage-clamp recordings different intra- and extracellular solutions and voltage-protocols were used. To record voltage gated sodium currents amplitude (I_{Na}) an external solution containing (in mM): 137 NaCl, 4 KCl, 1.8 CaCl₂, 1 MgCl₂, 10 HEPES-NaOH, 10 glucose, and 10 TEA-Cl (pH 7.4) was used while the intracellular pipette solution contained (in mM): 110 Cs gluconate, 3.7 NaCl, 5 MgCl₂, 10 HEPES, 5 EGTA and 5 Na₂ATP adjusted to pH 7.2 with CsOH. The external solution for potassium currents measurements contained (in mM): 119 NaCl, 5.9 KCl, 1 CaCl₂, 1.2 MgSO₄, 1.2 NaH₂PO₄, 22.8 NaHCO₃ and 0.1% glucose (pH 7.4 adjusted with CO₂ prior to use), while intracellular pipette solutions contained (in mM): 150 KCl, 2 MgCl₂, 5 HEPES, 1.1 EGTA and 2 Na₂ATP (pH 7.2). Unlike I_{Na} , voltage-gated potassium currents (I_K) were not studied in isolation, that is, after blocking the voltage-gated, inward Na⁺ current. This was done for two main reasons: first of all, I_{Na} provided a functional monitor of the recording conditions because it is very sensitive to variations in the series resistance associated with the patch electrode. An increase in series resistance can produce an artificial change in the amplitude of I_K . Second, I_{Na} did not interfere with the analysis of I_K amplitude, since I_{Na} inactivated completely in less than 10 ms after imposing the depolarizing steps to the membrane and I_K amplitude was always measured at the end of the voltage steps. The external and internal solutions for calcium measurements were designed to eliminate sodium and potassium channel currents. Thus, the bath solution contained (in mM) 110 NaCl, 25 TEA chloride, 5 4-AP, 5 CaCl₂, 10 HEPES, 1 MgCl₂, 5.4 KCl, 25 D-glucose, and 1 μ M TTX (pH 7.4). The electrode solution contained (in mM) 110 CsCl, 25 TEA chloride, 20 phosphocreatine, 50 units/ml phosphocreatine kinase, 10 EGTA, 10 HEPES, 5 NaCl, 2 MgCl₂, 0.5 CaCl₂, 0.5 BaCl₂,

2 Na₂ATP, and 0.1 NaGTP (pH 7.3). Gradual rundown of ionic currents over the recording time were occasionally observed, therefore those with > 1%/min rundown over the course of the experiment were excluded from the analysis. Moreover, all experiments were completed within 10 min, thus, rundown may have played only a minor role in our results.

Membrane potential was recorded in current-clamp mode using the intra- and extracellular solutions used for recording of potassium currents.

Determination of cytosolic calcium concentration ([Ca⁺²]_c) and intracellular pH (pH_i). Cell cultures of 5-7 days seeded onto 18 mm glass coverslips were washed twice with cold physiological saline solution supplemented with 0.1% bovine serum albumin (BSA). Saline solution was composed (in mM) by 119 NaCl, 5.9 KCl, 1 CaCl₂, 1.2 MgSO₄, 1.2 NaH₂PO₄, 22.8 NaHCO₃ and 0.1% glucose, (pH 7.4 adjusted with CO₂ prior to use). Cortical neurons were loaded with the calcium and pH sensitive dyes Fura-2 acetoxymethyl ester (Fura-2 AM) at a final concentration of 0.5 μM and 2',7'-bis(carboxyethyl)-5(6)-carboxyfluorescein acetoxymethyl ester (BCECF-AM, 0.5 μM) for 8 min at 37°C in the saline solution containing 0.1% BSA. After incubation, the loaded cells were washed three times with cold saline solution. The glass coverslips were inserted into a thermostated chamber at 37°C (Life Science Resources), and cells were viewed with a Nikon Diaphot 200 microscope, equipped with epifluorescence optics (Nikon 40x- immersion UV-Fluor objective). Addition of drugs was made by aspiration and addition of fresh bathing solution. The cytosolic calcium ratio was obtained from the images collected by a fluorescence equipment (Lambda-DG4, Sutter Instruments). The light source was a xenon arc bulb and the different wavelengths used were chosen with filters. The excitation wavelengths for Fura were 340 and 380 nm, and emission was collected at 505 nm. The experiments were performed in triplicate. The excitation wavelengths for BCECF were 440 and 490 nm and 530 nm for emission. The results of pH_i were expressed as a ratio of the emission fluorescence intensities 490/440; this ratio increases as pH_i rises. The 530 nm emission ratio resulting from 490/440 excitation was converted into a linear pH scale by means of in situ calibration between pH 6 and pH 9 performed when necessary using the nigericin technique.¹⁹

Toxins and drugs used. CTX 3C was synthesized following previously described procedures²⁶,²⁷ and dissolved at a concentration of 10 μM in DMSO. Following dilutions were performed in deionized water. MTX was generously provided by Prof. Yasumoto. Tetrodotoxin (TTX) was purchased from CIFGA (Lugo, Spain). All toxins had purity higher than 99%. The final

concentration of compound solvent (DMSO), was less than 0.01%. All other chemicals were reagent grade and purchased from Sigma.

Statistical Analysis. All data are expressed as means \pm SEM of n determinations. Statistical comparison was by paired Student's t test. P values < 0.05 were considered statistically significant.

Results

The most notable feature, common to all ciguatoxins, is the long semi-rigid architecture so-called ladder-shaped polyether (LSP) that comprises fused ether rings of various sizes. Other toxins such as brevetoxins and MTX are structurally-related toxins. Whereas CTX and brevetoxins have a similar molecular size, MTX is the largest (3 times) with 32 cyclic ethers. Figure 1 shows the chemical structures of CTX 3C and MTX as well as their 2D structure, obtained employing the VEGA Program.²⁸ MTX backbone is amphiphilic and can be divided into both hydrophobic (absence of enough structural polar moieties) and hydrophilic (sulphate and hydroxyl moieties) regions. This amphipathic nature resembles bile salts structures which bind to the cell membrane owing to its amphipathic nature. Whereas CTX 3C is a clearly lipophilic molecule, the overall lipophilicity of MTX is reduced since the heterogeneity of the distribution of this lipophilicity is higher than in the other ones. The first region of MTX resembles the CTX 3C backbone not only by its relatively lipophilic character but also by the presence of a nine-membered ring, the molecular size and the rigid conformation with an extended form, which is long enough to span lipid bilayer membranes.¹³ Meanwhile, the relatively hydrophilic backbone of MTX shows a more flexible orientation and is depicted by polyhydroxy groups, similar to palytoxins (composed basically by acyclic polyol moieties) and, both are considered as huge polyol molecules (more than 100 Å in length). Since these huge molecules could assume several conformations, their three-dimensional structures could play an essential role in their interaction with biomacromolecules.²⁹

As part of the structure of MTX resembles to that of CTX 3C, it could be expected that both toxins share similar effects in the context of a common cellular model. Therefore, we used a wide range of techniques, including cellular viability, intracellular calcium and pH imaging, and whole cell patch clamp in order to better understand the effects of these toxins in neurons. First

the effects of CTX 3C and MTX on voltage-gated channels in mouse cortical neurons were evaluated.

Effects of CTX 3C and MTX on voltage-gated sodium channels

Since ciguatoxins interact with voltage-gated sodium channels, first the effect of both toxins on sodium channel activation was analyzed (Figure 2). Voltage-dependent sodium currents were elicited in cortical neurons by applying a series of 25 ms depolarizing pulses (voltage steps), in 5 mV increments, from a holding potential of -100 mV.²⁴ The sensitivity of these currents to TTX is shown in Supplementary Figure 1. Figure 2A shows the current-voltage (I-V) relationships for the effect of CTX 3C on VGSCs in neurons cultured for 10-12 days *in vitro* (div). Bath application of different concentrations of the toxin caused a concentration-dependent decrease on sodium current amplitude. While 0.01 nM and 0.1 nM CTX 3C did not modify inward sodium current amplitude (n = 3 and n=8 cells, respectively), normalized peak I_{Na} decreased by $14.5 \pm 0.06\%$ (p < 0.05; n = 6) and $30.4 \pm 0.04\%$ (p < 0.001; n=3) in the presence of 1 nM and 5 nM CTX 3C, respectively. Moreover, the activation of sodium channels was shifted in the hyperpolarizing direction after bath application of CTX 3C. Bath application of 1 and 5 nM CTX3C, shifted the activation threshold of sodium current, from -53.6 ± 1.8 mV (n = 7) in control conditions to -68.3 ± 3.6 mV (n = 6; p = 0.001) after bath application of 1 nM CTX 3C and to -75.0 ± 5 mV (n = 3; p = 0.0004) after addition of 5nM CTX 3C. The percent of inhibition of the peak inward sodium currents by different concentrations of this toxin was used to obtain a concentration-response curve, as shown in Figure 2B. Nonlinear fit of the data in Figure 2B yielded an estimated IC_{50} (95 % confidence interval) for the CTX 3C inhibition of peak I_{Na} of 7.1×10^{-9} M (4.5×10^{-9} M to 11.3×10^{-9} M). Since at 10-12 div cortical neurons show many large neuronal processes, additional experiments were performed using younger neurons to exclude an effect of a possible space clamp error in these results. As shown in Figure 2C, using cultures of 5-6 div, the effect of CTX 3C in the activation potential of sodium channels was even largely shifted in the hyperpolarizing direction. In this case, the activation potential of sodium channels was -44.3 ± 3.2 mV (n = 7) in control neurons, -61.4 ± 2.4 mV in the presence of 1 nM CTX 3C (n = 7; p < 0.001), and -78.7 ± 1.2 mV (n = 4; p < 0.001) after bath application of 5 nM CTX 3C. Similarly peak sodium current was not affected by 1 nM CTX 3C but it was decreased by $42.4 \pm 8.3 \%$ (p < 0.001) in the presence of 5 nM CTX 3C.

Little is known about the effects of MTX on VGSC, since most studies have focused on the MTX-induced activation of calcium influx. In cortical neurons of 10-12 div, 1 nM MTX did not elicit a significant change in the peak amplitude of sodium currents as shown in the I-V curve of sodium channel activation (Figure 2D). Moreover, MTX slightly shifted the activation of VGSC in the hyperpolarizing direction from -45.0 ± 2.7 mV in control conditions to -52.0 ± 4.3 mV ($n = 5$), although this result did not reach statistical significance. Additionally, a higher concentration of maitotoxin, 5 nM, was evaluated to exclude possible space-clamp errors in the results. As shown in Figure 2E, in 5-6 div cortical neurons, bath application of 5 nM MTX did not modify the activation potential of voltage-dependent sodium channels, which was -40.0 ± 3.6 mV in control conditions and -43.3 ± 4.4 mV in the presence of 5 nM MTX ($n = 6$; $p = 0.28$) but it decreased the peak sodium current amplitude by 27.9 ± 11.0 % ($n = 6$; $p = 0.02$). Representative voltage dependent sodium currents at a test potential of -20 mV in the absence and presence of 5 nM CTX 3C or 5 nM MTX are shown in Figure 2F.

We further studied the effect of CTX 3C and MTX in the voltage dependence of steady-state inactivation of sodium channels (Figure 3). Depolarization induces VGSC inactivation that prevents the immediate re-opening of VGSC, and the channels normally require several milliseconds to fully recover their excitability.³⁰ To study the effect of MTX and CTX 3C on sodium channel inactivation, a typical two-pulse voltage protocol (prepulse and test pulse) that allowed the evaluation of the non inactivated fraction of the sodium current as a function of the prepulse membrane potential was used (Figure 3 inset). Steady-state inactivation curves showed that in the presence of 5 nM CTX 3C (but not at lower concentrations), inactivation was shifted by nearly 30 mV in the hyperpolarizing direction (Figure 3A). Half inactivation voltage values ($V_{inact1/2}$) were -48.7 ± 6.1 mV ($n = 8$) in control conditions, -51.1 ± 7.6 mV ($n = 7$) in the presence of 1 nM CTX 3C and -82.9 ± 1.5 mV ($n = 4$) after bath application of 5 nM CTX 3C, indicating that at any given membrane potential the fraction of inactivated channels was larger when 5 nM CTX 3C was added to the bath solution. In the same conditions, MTX caused only a small hyperpolarizing shift in the inactivation curve of sodium channels (Figure 3B). Half inactivation voltage values ($V_{inact1/2}$) were -59.0 ± 8.0 mV in control conditions and -69.9 ± 16.9 mV ($n = 6$) in the presence of 1 nM MTX, although this difference did not reach statistical significance. Therefore, additional experiments were performed using 5 nM MTX. In this case,

Vinact_{1/2} was -58.9 ± 10.9 mV in control cells and -70.9 ± 18.9 mV in the presence of 5 nM MTX (n = 7; p = 0.079) as shown in Figure 3B.

CTX 3C and MTX do not affect potassium current amplitude in cortical neurons

Next, the effects of CTX 3C and MTX on the amplitude of voltage-gated potassium channels (I_K) was evaluated (Figure 4). Although there are no reports regarding the effects of MTX on potassium channels amplitude, CTX 3C has been reported not to modify potassium channels in mouse taste cells.³¹ However, other toxins produced by *Gambierdiscus toxicus* such as gambierol have been implicated in regulating these channels.³² To measure the effect of the toxins on potassium current amplitude, neurons were voltage clamped at a membrane holding potential of -60 mV, and total potassium currents were evoked by 200 ms depolarizing pulses from V_m to +75 mV in 15 mV steps (Figure 4, inset). Neither 5 nM CTX 3C (n = 7) nor 1 nM MTX (n = 8), affected potassium currents in cortical neurons (Figures 4A and 4B, respectively). Moreover, the activation threshold for I_K (about -45 mV) was not affected by these toxins. Since we did not study potassium currents in isolation, during the course of these experiments we noticed that, in some cells 5 nM CTX 3C produced spontaneous sodium currents at holding potentials of -60 mV (Figure 4C). These currents were partially blocked by TTX (Figure 4 C), however this was not observed in the presence of 1 nM MTX (Figure 4 D).

Neither CTX 3C nor MTX affected voltage gated calcium channels in cortical neurons

There is little information relating the activity of MTX and CTX 3C on voltage gated calcium channels (VGCC). Although it has been proposed that MTX may alter the voltage dependence of calcium channel activation, the direct effects of maitotoxin on VGCC were not directly tested in that previous study.³³ Voltage dependent calcium currents were elicited by 20 mV depolarizing steps from -70 mV to +20 mV in 10 mV increments. Holding potential was -80 mV (2 s prepulse). Inward currents were normally activated at voltages more positive than -50 mV and peaked between -10 and 0 mV. CTX 3C, at 5 nM, did not alter the I-V curve of VGCCs (Figure 5A, left panel) nor the average peak amplitude of calcium currents, measured at 0 mV, as shown in the middle panel. The right panel in Figure 5A shows representative Ca^{+2} current traces before and after the addition of 5 nM CTX 3C and the CTX 3C sensitive current obtained by subtracting the CTX 3C current from the control current. Similarly, MTX did not modify VGCC activation

as shown in the IV-curves obtained after bath application of 1 nM and 5 nM MTX, shown in Figure 5B (left and right panel, respectively). Figure 5C shows the normalized average calcium currents amplitudes in control conditions and in the presence of 1 nM MTX or 5 nM MTX which were -221.2 ± 59.9 pA in control conditions and -173.7 ± 39.5 pA in the presence of 1 nM MTX ($n = 4$), while in cells treated with 5 nM MTX peak I_{Ca} was -197.7 ± 39.7 pA in the absence of toxin and -192.8 ± 35.5 pA after bath application of 5 nM MTX ($n = 3$). Representative calcium current traces before and after addition of 1 nM MTX as well as the MTX sensitive current are shown in the right panel of Figure 5C.

In order to complete the analysis of the effect of both toxins on VGCC, their action on channel inactivation was evaluated. The voltage dependence of the inactivation of VGCC is based mainly on the voltage dependency of activation because inactivation depends primarily on the state of the channel, rather than on voltage.³⁴ To study the kinetics of the VGCC inactivation, calcium currents were generated by a 200 ms test pulse (TP) to +10 mV preceded by a 1.5-s conditioning prepulse (CP) from -80 to +10 mV in 10 mV increments (Figure 6, inset). Currents, elicited from the TP and the CP, were normalized to the current associated with their maximal current. The maximal rate of inactivation occurred near the peak of the I-V curve, between 0 and +10 mV, either in control conditions or in the presence of 5 nM CTX 3C or 1 nM MTX (Figure 6A and 6B, respectively). Normalized current amplitude against the CP potential was fitted by the Boltzman equation. Steady state inactivation yielded a $V_{1/2}$ of -37.7 ± 1.8 mV in control conditions and -36.9 ± 3.1 mV in the presence of 5 nM CTX 3C ($n = 5$). Similarly, maitotoxin did not affect the inactivation curve obtaining a $V_{1/2}$ of -39.5 ± 2.1 mV in control conditions and -44.3 ± 5.2 mV in the presence of 1 nM MTX ($n = 3$). Figure 6C and 6D show representative current traces in the absence (control) and presence of 5 nM CTX 3C or 1 nM MTX, respectively, at CP of 0 and -80 mV. In both cases, CP to very negative voltages, starting at -80 mV, evoked minimal calcium currents and yielded near maximal calcium currents on the test pulse. By contrast, a CP to the maximum of calcium current activation (about 0 mV) evoked maximal calcium currents and resulted in a minimal current on the test pulse, produced as a result of calcium channel inactivation, which was unaltered by CTX 3C or MTX.

In summary, the electrophysiological evaluation of the effects of CTX 3C and MTX in cortical neurons, indicated that both compounds lacked an effect on voltage gated potassium and calcium channels, however, CTX 3C shifted the activation threshold and the inactivation curve of voltage

gated sodium channels to more hyperpolarizing potentials, while, at the same concentrations, MTX did not have a significant effect on VGSC.

MTX, but not CTX 3C, caused cell death in cortical neurons

Next, the *in vitro* toxicity of CTX 3C and MTX in cortical neurons was evaluated using the MTT assay. The effect of these compounds on cell viability was assessed after 24 hours exposure of cortical neurons to CTX 3C at concentrations ranging from 0.01 nM to 10 nM or to MTX at concentrations from 0.001 to 1 nM. As indicated in Figure 7A, CTX 3C did not produce a cytotoxic effect at any of the concentrations studied, which is in agreement with other studies.³⁵ However, in cortical neurons, 24 hours exposure to MTX caused a concentration- dependent decrease in cell viability, causing complete cell death at 1 nM. As shown in Figure 7B, nonlinear fit of the effect of MTX on cell viability yielded an estimated IC₅₀ (95 % confidence intervals) of 0.12 nM (8.1 x 10⁻¹¹ M to 1.9 x 10⁻¹⁰ M). Although, previous studies reported total cell death of cortical neurons after exposure to 0.1 nM MTX²¹ the type of cellular viability assay may account for this difference.

MTX, but not CTX 3C, triggers a rapid rise in cytosolic Ca⁺², intracellular acidification and cytotoxicity in cortical neurons

Intracellular calcium plays a crucial role in regulating neuronal excitability, release of transmitters, synaptic plasticity, and apoptosis.³⁶⁻³⁸ Ciguatoxin, at higher concentrations than those employed in this work, has been described to promote the mobilization of intracellular Ca⁺² secondary to Na⁺ influx through VGSC in neuroblastoma cells and to stimulate the inositol 1,4,5 triphosphate-releasable Ca⁺² store,¹¹ while the main effect of MTX in several cellular models is to produce a massive calcium influx^{15, 16} leading to cell death. As indicated in Figure 8A, in a Ca⁺²-free medium, 5 nM CTX 3C did not produce any effect thus indicating that the intracellular Ca⁺² stores were not affected by the toxin. In addition, the toxin did not modify the cytosolic calcium levels even when 1 mM Ca⁺² was added to the extracellular media (left panel). Since CTX effects on cytosolic calcium could be transient additional experiments were performed adding CTX 3C at 5 or 10 nM in calcium-containing media. As shown on Figure 8B, in these conditions CTX 3C did not modify cytosolic calcium levels, nor the intracellular pH as shown in Figure 8C. Similarly, maitotoxin at 1 nM did not modify the cytosolic calcium concentration in a Ca⁺²-free medium (data not shown), in agreement with previous studies.³⁹

However, in the presence of 1 mM Ca^{+2} in the bathing solution, MTX induced a rapid and concentration-dependent Ca^{+2} influx (Figure 8D). At 0.1 nM and 1 nM, MTX significantly enhanced the $[\text{Ca}^{+2}]_c$ by $34.5 \pm 2.2\%$ ($n = 4$, $p < 0.001$) and $39.9 \pm 3.7\%$ ($n = 4$, $p < 0.001$), respectively, two minutes after bath addition of the toxin. However, this effect did not reach statistical significance for the lowest concentration of MTX, 0.01 nM. It has been reported that lowering extracellular pH decreases the MTX-dependent calcium influx,^{21, 22} however as far as we know, the effect of the toxin on intracellular pH has not been previously evaluated. Since other phycotoxins such as palytoxin (PTX), have been reported to induce a rapid rise in calcium which was associated with a decrease in intracellular pH,²⁰ the effect of MTX on intracellular pH was tested in cortical neurons. The resting pH_i values in cortical neurons were 7.2 ± 0.02 ($n = 4$). These values were similar to those previously described for neuronal cells in our laboratory.¹⁹ As shown in Figure 8E, MTX at 0.1 and 1 nM produced a rapid acidification in cortical neurons. When measured two minutes after the addition of different concentrations of MTX, 0.01 nM MTX did not significantly modify pH_i which was 7.2 ± 0.01 ($n = 4$; $p = 0.13$). However, bath application of 0.1 nM and 1 nM MTX decreased pH_i to 7.0 ± 0.03 ($n = 4$, $p = 0.001$) and 6.97 ± 0.06 ($n = 4$; $p < 0.05$), respectively.

In order to see if the rapid effects of MTX on the cytosolic calcium concentration and intracellular pH altered neuronal viability in a short time scale, cortical neurons were exposed to different concentrations of MTX for 10 min and then cellular viability was assessed. Figure 8E shows the effect of a 10 min exposure of cortical neurons to 0.1 and 1 nM MTX on cell viability. Treatment of neurons with 0.1 nM MTX during 10 min decreased cell viability by about 15% of control values ($p < 0.01$), whereas a 10 min exposure of cortical neurons to 1 nM MTX decreased cell viability by about 37% of control values ($p < 0.01$). These results constitute the first evidence that the cytotoxicity induced by MTX is initiated very rapidly after exposure of the neurons to the toxin.

MTX-induced depolarization, intracellular calcium influx and acidification in cortical neurons is ameliorated by blockade of voltage-gated sodium channels

Both ciguatoxins and maitotoxins are known to produce membrane depolarization.^{23, 40} Since, we have previously found that CTX 3C causes a tetrodotoxin-sensitive cell depolarization in cortical neurons (manuscript in preparation), we evaluated the effect of MTX on membrane

depolarization. Under current clamp conditions, average resting potential (V_m), was significantly depolarized from -50.0 ± 1.3 mV in control conditions to -35.3 ± 4.3 mV ($p = 0.003$; $n = 7$) in the presence of 1 nM MTX (Figure 9A, left panel). This effect was partially suppressed by the addition of 0.5 μ M TTX to the bath solution (Fig 9A, right panel). In this case, the values of the resting potential in control conditions (in the presence of TTX) were -53.5 ± 2.6 mV and -43.4 ± 2.4 mV ($p = 0.01$; $n = 5$) in the presence of 1 nM MTX, however not significant differences were found in the resting membrane potential recorded in the presence of MTX alone or in the presence of MTX + TTX ($p = 0.09$). Thus, the results presented here suggest that the membrane depolarization elicited by MTX was not primarily mediated through VGSC, however voltage-gated sodium channels activation is probably secondary to the large calcium influx caused by the toxin in cortical neurons.

We further investigated whether voltage-gated sodium channels could contribute to the MTX induced increase in cytosolic calcium, acidification and cytotoxicity in cultured neurons. Assuming that the MTX-induced neuronal depolarization could lead to a subsequent increase in $[Ca^{+2}]_c$, we investigated the effect of the VGSC blocker TTX on the MTX-induced $[Ca^{+2}]_c$ increase. As indicated in Figure 9B, 10 minutes preincubation of cortical neurons with 100 nM TTX before addition of 0.1 nM MTX delayed the onset of the MTX-induced rise in $[Ca^{+2}]_c$ by about 40 seconds and modified the profile of the rise in calcium caused by MTX, generating a progressive increase in calcium influx. TTX did not modify the basal calcium levels. Furthermore, 10 minutes preincubation of neurons with 100 nM TTX (Figure 9C) significantly reduced the acidification caused by 0.1 nM MTX ($p < 0.05$), again indicating that voltage-gated sodium channels could contribute to the cellular effects caused by MTX.

Taking into account these results, the possible relationship between the MTX-induced calcium increase, intracellular acidification, voltage-gated sodium channels, and MTX cytotoxicity in cultured cortical neurons was evaluated. In order to do this, cortical neurons were exposed to 0.1 nM MTX either during 24 h or during 10 minutes in the absence and presence of the VGSC blocker TTX (0.5 μ M). As shown in Figure 9D, TTX reduced only the cytotoxic effect of MTX by $8.1 \pm 2.8\%$ ($p < 0.05$) after 24 h exposure. In contrast, the cytotoxicity elicited by 10 min exposure of cortical neurons to MTX was completely reverted in the presence of TTX, therefore indicating that the initial and rapid cytotoxic effect of MTX in cortical neurons involves mechanisms related with tetrodotoxin-sensitive voltage-gated sodium channels.

The results presented in this paper clearly indicate novel cellular effects of MTX in cortical neurons showing that sodium channel blockade ameliorates the MTX-induced calcium influx and acidification in neurons which cause cell death. However, our results indicate that the protective effect of voltage-gated sodium channel blockers on MTX induced toxicity may be temporal since this effect was evident when the neurons were treated with MTX during 10 min but had a minor contribution after 24 hours exposure of cortical neurons to MTX.

Discussion

In excitable cells ciguatoxins induce membrane depolarization which is known to be due to the ability of these toxins to increase Na⁺ influx through VGSC.²³ As expected, in cortical neurons and under voltage clamp conditions CTX 3C elicited a hyperpolarizing shift in the activation potential of VGSC and also reduced peak sodium inward current, similarly to the effects previously described in other cell types.^{30,31} On the other hand, there is evidence in the literature that MTX modulates ion channels. In some cell types, MTX appears to activate VGCC.^{33,41,42} In other cells lacking these channels, MTX activates non-selective channels.¹⁶ Moreover, there is a lack of information regarding the effects of MTX on voltage gated sodium channels since most of the studies evaluating the cellular actions of MTX were focused on the calcium influx produced by this toxin. Interestingly, in cortical neurons, MTX affected VGSC decreasing peak sodium current amplitude, an effect similar to that elicited by CTX 3C. Although the mechanisms underlying the decrease in sodium current amplitude elicited by 5 nM MTX have not been addressed in this study, it is likely due to the calcium-dependent inactivation of sodium channels elicited by the calcium rise, as previously reported in other neurons.⁴³

We have recently shown that CTX 3C causes membrane depolarization in cortical neurons and that this effect was abolished by TTX (manuscript in preparation). Interestingly, here we observed that MTX also produces membrane depolarization in cortical neurons which is probably related with the calcium influx elicited by the toxin. However, in contrast with our recent results with CTX3C, this action was not fully blocked by TTX. Thus, we suggest that MTX could depolarize cortical neurons by other mechanisms independent of VGSC as it has been previously reported in other cell types.³³

Under voltage clamp conditions, neither 5 nM CTX 3C nor 1 nM MTX, altered voltage-gated potassium currents in mouse cortical neurons. Regarding the effect of CTX 3C on potassium

channels, the results presented here are in agreement with previous studies where CTX 3C did not modulate voltage-gated potassium channels in mouse taste cells.³¹ However, the same toxin decreased potassium currents in cerebellar granule cells,⁴⁴ and other ciguatoxins such as P-CTX-1 (20 nM) blocked voltage-gated potassium channels in rat myotubes⁴⁵ and rat sensory neurons.⁴⁶ These differences may be due to a different expression of potassium channels subtypes in these cellular systems or to differences between the experimental conditions since in this work the effect of the toxin on potassium currents was evaluated in the absence of VGSC blockers.

Although the direct effect of ciguatoxins on VGCC had never been presented, Molgó et al. reported that some ciguatoxins such as P-CTX-1 (5-25 nM), increase intracellular Ca^{+2} concentration in neuroblastoma x glioma hybrid cells bathed both in a medium containing calcium or in a Ca^{+2} -free medium.⁴⁷ They suggested that this action was dependent on Na^{+} influx through VGSC since TTX prevented the CTX-induced calcium mobilization. Later, the authors suggested that P-CTX-1 elevated intracellular calcium through an inositol 1,4,5-triphosphate pathway.¹¹ The same group reported a similar effect of 10 nM P-CTX-1B in rat myotubes.⁴⁵ However, in our experimental conditions, CTX 3C did not directly affect VGCC and did not trigger calcium influx into the cells neither in a Ca^{+2} -free media or in a media containing 1 mM Ca^{+2} . Again, the discrepancies found between the absence of effects of CTX 3C on intracellular Ca^{+2} concentration in cortical neurons and the effects of P-CTX-1 on intracellular Ca^{+2} concentration in other cellular models previously reported¹¹ may be a consequence of the different types of toxins and cells employed.

On the other hand, it is broadly known that MTX produces a massive calcium influx to the cell leading to cell death. However, there is a wide controversy according to its mechanism of action. Up to date, the MTX- induced Ca^{+2} influx has been related to a very wide range of targets such as non-selective cation channels,^{48, 49} voltage-gated calcium channels,^{15, 41, 50} receptor operated Ca^{+2} channels^{51, 52} and to the sodium/calcium exchanger operating in reverse mode.⁵³ Regarding VGCC, it has been described that in neuroblastoma x glioma hybrid cells and pituitary tumor cells, L- type VGCC were involved in the MTX-elicited Ca^{+2} influx.¹⁵ In contrast, in other cell types such as smooth muscle BC3H1 cells¹⁷ and synaptosomes,¹⁸ calcium channel antagonists had no effect on the MTX-elicited Ca^{+2} influx. However, a direct electrophysiological evaluation of the effects of MTX on VGCC has never been described. In our experimental conditions, MTX induced a rapid rise in cytosolic calcium in calcium containing medium but not in a calcium-free

medium, thus excluding an effect of the toxin on intracellular calcium stores at the toxin concentrations evaluated in this work. However, neither CTX 3C, nor MTX affected the activation and inactivation properties of VGCC, neither the calcium current amplitude in cortical neurons.

It has recently been shown that MTX activates the sodium/hydrogen exchanger in primary cultures of rat cortical neurons, causing intracellular sodium increase, reverse operation of the sodium/hydrogen exchanger and calcium influx, although the mechanisms underlying the reverse operation of the sodium hydrogen exchanger were not identified.²¹ Moreover, it has been recently demonstrated that a decrease in pH_i causes toxic Ca^{+2} entry through coactivation of the sodium/calcium exchanger and the sodium/hydrogen exchanger in neuroblastoma cells.⁵⁴ However, the MTX effects in intracellular pH had not been described previously. The results presented here indicate that MTX causes a concentration-dependent calcium influx and simultaneous intracellular acidification in cortical neurons which may exacerbate the MTX-induced cytotoxicity in this cellular model. Since, intracellular pH is probably the most important physiological factor regulating the sodium/hydrogen exchanger⁵⁵ it is likely that the MTX-induced activation of the sodium/hydrogen exchanger previously reported²¹ may be the result of a cellular mechanism to compensate the MTX-induced intracellular acidification. Interestingly, blockade of VGSC delayed the MTX-induced rise in cytosolic calcium and intracellular acidification as well as the cytotoxic effect elicited after 10 minutes exposure to the toxin. In this sense, it is noteworthy that VGSC have been previously described to be involved in the calcium influx elicited by other neurotoxins such as PTX,¹⁹ which also induces intracellular acidification and decreases cell survival in neurons.⁵⁶ Therefore, the results presented here indicate that the intracellular acidosis caused by MTX in cortical neurons, could aggravate the cytotoxicity of this powerful marine phycotoxin.

In summary, the major differences regarding the effects of CTX 3C and MTX in cortical neurons were the massive calcium influx and intracellular acidification leading to neuronal death produced by MTX and not by CTX 3C. Interestingly, we found several analogies among both toxins. Despite any of them affected voltage gated calcium or potassium channels, MTX also decreased peak sodium currents, as it was broadly reported for CTX 3C. Indeed, blockade of VGSC reduced MTX-dependent calcium influx, acidification and neurotoxicity. We hypothesize

that the analogies and differences in the bioactivity of these two toxins produced by the same microorganism may be strongly linked to their chemical structure. Although these compounds share a common biosynthetic pathway and a similar lipophilic region on their structure, MTX is structurally more complex than CTX. Considering the chemical structure, we could attribute the biofunctional differences observed here to the huge and more amphiphilic character of MTX. Thus, it would be interesting to isolate the hydrophilic and lipophilic regions of MTX in order to elucidate if the hydrophilic fragment of MTX is the responsible for calcium influx, intracellular acidification and neurotoxicity.

FIGURE LEGENDS

Figure 1. Ciguatoxin and Maitotoxin structures. **A**, MTX chemical and 2D structure. CTX like moiety (hydrophobicity, size and nine-membered ring) is highlighted. **B**, CTX 3C chemical and 2D structure. Molecular Lipophilic Potential Surface was created using a color ramp (gradient) in which the black color and the white colors are the boundaries of the more hydrophilic and more lipophilic character, respectively.

Figure 2. Effect of CTX 3C and MTX on voltage-gated sodium channels activation in cortical neurons. **A**, I-V relationship for the effect of different concentrations of CTX 3C on sodium currents in cortical neurons of 10-12 div. Note that 5 nM CTX 3C induced a marked reduction of peak I_{Na} . **B**, concentration-response graph indicating the effect of CTX 3C on peak I_{Na} . **C**, I-V relationship for the effect of 1 and 5 nM CTX 3C on sodium currents in cortical neurons of 5-6 div. **D**, I-V relationship for the effect of 1 nM MTX on sodium currents in cortical neurons of 10-12 div. **E**, I-V relationship for the effect of 5 nM MTX on sodium currents in cortical neurons of 5-6 div. **F**, representative peak sodium currents in the absence of toxin and in the presence of 5 nM CTX 3C or 5 nM MTX.

Figure 3. Effect of CTX 3C and MTX on the voltage dependence of the steady state inactivation of sodium channels. Steady-state inactivation was determined using the two-pulse protocol shown (inset). A 500 ms conditioning prepulse from -120 to 15 mV was stepped in 15 mV increments and followed by a 50 ms test pulse to -20 mV. **A**, Effect of CTX 3C on sodium channel inactivation. Half maximal inactivation voltage ($V_{1/2}$) remained unaltered during

application of 1 nM CTX 3C but it was shifted by more than 30 mV in the negative direction by 5 nM CTX 3C (n = 4). **B**, MTX, at 5 nM, did not have a significant effect on the steady-state inactivation of sodium channels. All currents were normalized to the maximum control current. Curves were fitted to Boltzman equation.

Figure 4. Effect of CTX 3C and MTX on voltage-gated potassium channels. Neurons were voltage clamped at a membrane holding potential (V_h) of -60 mV and I_K was evoked by a 200 ms depolarizing pulse from the holding membrane potential to +75 mV in 15 mV steps (inset). **A**, I-V relationship for I_K recorded in the absence (control) and presence of 5 nM CTX 3C (n = 7). **B**, I-V relationship for I_K recorded in the absence (control) and presence of 1 nM MTX (n = 8). **C**, representative recording from a single cortical neuron. Whole-cell currents consisted of voltage-gated sodium currents (downward deflection in the current recording) and voltage-gated potassium currents. Application of 5 nM CTX 3C did not affect I_K , however it considerably inhibited I_{Na} producing spontaneous currents at V_m of -60 mV that were partially blocked by TTX. Detailed spontaneous currents at V_m of -60 mV are shown in the right panel of C. **D**, representative recording from a single cortical neuron before and after the addition of 1 nM MTX.

Figure 5. Effect of CTX 3C and MTX on voltage-gated calcium currents. **A**, The I-V relationship for calcium currents amplitude (I_{Ca}) normalized to the maximum current amplitude (I_{max}) in the absence and presence of 5 nM CTX 3C, is shown on the left. Neurons were voltage clamped at a holding potential of -65 mV and I_{Ca} was evoked by 200 ms depolarizing voltage steps ranging from -70 to +20 mV in 10 mV increments preceded by a 2 s prepulse to -80 mV (inset). Pooled results of I_{Ca} measured at 0 mV (peak) in the absence (control) and presence of 5 nM CTX 3C are shown in the middle. The right panel shows representative traces of peak Ca^{+2} currents evoked at 0 mV in the absence (control) and presence of 5 nM CTX 3C. Note that the CTX 3C-sensitive calcium current was null (right panel). **B**, I-V relationship of I_{Ca} normalized to the I_{max} in the presence and absence of 1 nM MTX (left panel) or 5 nM MTX (right panel). **C**, pooled results of I_{Ca} measured at 0 mV in the absence (control) and presence of 1 nM or 5 nM MTX are shown in the left. The number of cells is indicated in parentheses The right panel shows representative traces of peak calcium currents evoked at 0 mV in the absence (control)

and presence of 1 nM MTX. Note that the MTX-sensitive calcium current was null (lower panel). Sensitive currents were obtained by subtracting the current after the application of the toxin from the control current.

Figure 6. Voltage dependence of the steady state inactivation of VGCC in the absence and presence of CTX 3C or MTX. Current amplitudes were normalized to the maximum current (I_{max}). Inset, inactivation pulse protocol: a 200 ms test-pulse (TP) to 10 mV was preceded by a 1.5 s conditioning prepulse (CP). Voltage steps ranged from -80 to +10 mV in 10 mV increments. V_m was -65 mV. **A** and **B**, I-V relationship of steady state inactivation for 5 nM CTX 3C (**A**) and 1 nM MTX (**B**), ($n = 3$ & $n = 5$ respectively). **C** and **D**, representative steady state inactivation calcium current traces in the absence (control) and presence of 5 nM CTX 3C (**C**) or 1 nM MTX (**D**) at conditioning pulses of 0 and -80 mV.

Figure 7. Toxicity of CTX 3C and MTX in cortical neurons. **A**, Twenty four hours exposure of cortical neurons to CTX 3C did not modify cell viability. **B**, Twenty four hours exposure of cortical neurons to MTX induced cell death in a concentration-dependent manner, assayed using the MTT assay. Experiments were performed in triplicate from 5 different cultures.

Figure 8. CTX 3C and MTX effects on cytosolic calcium concentration and intracellular pH. **A**, Acute addition of 5 nM CTX 3C did not produce calcium influx in a calcium-free medium. **B**, Bath application of 5 and 10 nM CTX 3C in a calcium-containing medium did not modify basal calcium levels in cortical neurons. **C**, Bath application of 5 and 10 nM CTX 3C did not modify intracellular pH in cortical neurons. **D**, Acute addition of MTX produced intracellular calcium influx in a concentration dependent manner. **E**, Bath application of 0.1 nM and 1 nM MTX produced intracellular acidification in a concentration dependent manner. **F**, Ten minutes exposure of cortical neurons to 0.1 or 1 nM MTX significantly reduced cellular viability as evaluated using the MTT assay. Experiments were performed in triplicate.

Figure 9. Blockade of VGSC are involved in the MTX effects in cortical neurons. **A**, acute addition of 1 nM MTX depolarizes the resting potential of cortical neurons in the absence and presence of TTX, left and right panel respectively. The number of cells tested is indicated in parentheses. **B**, 10 min preincubation of cortical neurons with 100 nM tetrodotoxin decreased the MTX-induced rise in $[Ca^{+2}]_c$. **C**, 10 min preincubation of cortical neurons with 100 nM tetrodotoxin decreased the MTX-induced acidification. Experiments were performed from 3 different cultures. MTX was added at the time points indicated by the arrows. **D**, 10 min

preincubation of cortical neurons with 500 nM tetrodotoxin slightly reduced the toxicity elicited by 0.1 nM MTX after 24 h treatment (left panel) but it completely reverted the cytotoxic effect of 0.1 nM MTX after 10 min exposure of cortical neurons to the toxin (right panel).

Corresponding Author

* Luis M Botana. E-mail: luis.botana@usc.es. Phone/Fax: +34982822233.

*Carmen Vale. E-mail: mdelcarmen.vale@usc.es.

Departamento de Farmacología, Facultad de Veterinaria, Universidad de Santiago de Compostela, Campus Universitario s/n, 27002, Lugo.

Author Contributions

The manuscript was written through contributions of all authors. All authors have given approval to the final version of the manuscript.

ACKNOWLEDGMENT

The research leading to these results has received funding from the following FEDER cofunded-grants: From Ministerio de Ciencia y Tecnología, Spain: AGL2009-13581-CO2-01, AGL2012-40485-CO2-01. From Xunta de Galicia, Spain: 10PXIB261254 PR. From the European Union's Seventh Framework Programme managed by REA-Research Executive Agency <http://ec.europa.eu/research/rea> (FP7/2007-2013) under grant agreement Nos. 211326-CP (CONFIDENCE), 265896 BAMMBO, 265409 μ AQUA, and 262649 BEADS, 315285 Ciguatools and 312184 PharmaSea. From the Atlantic Area Programme (Interreg IVB Transnational): 2009-1/117 Pharmatlantic.

Supporting information: Supplementary Figure 1. This information is available free of charge via the internet at <http://pubs.acs.org/>.

The authors wish to thank Prof. T. Yasumoto for generously providing us purified Maitotoxin.

ABBREVIATIONS

MTX, maitotoxin; CTX, ciguatoxin; VGSC, voltage gated sodium channel; VGCC, voltage gated calcium channel; NHX, sodium hydrogen exchanger; MTT, (3-[4,5-dimethylthiazol-2-yl]-2,5-diphenyltetrazolium bromide) test; I_{Na} , voltage gated sodium current amplitude; I_K voltage-gated potassium current amplitude; I_{Ca} , voltage gated calcium current amplitude; pH_i, intracellular pH; $[Ca^{2+}]_c$, cytosolic calcium concentration; TTX, tetrodotoxin; LSP, ladder-shaped polyether.

REFERENCES

- (1) Bagnis, R., Kuberski, T., and Laugier, S. (1979) Clinical observations on 3,009 cases of ciguatera (fish poisoning) in the South Pacific. *Am. J. Trop. Med. Hyg.* 28, 1067-1073.
- (2) Watters, M. R. (1995) Organic neurotoxins in seafoods. *Clin. Neurol. Neurosurg.* 97, 119-124.
- (3) Lewis, R. J. (2001) The changing face of ciguatera. *Toxicon* 39, 97-106.
- (4) Pearn, J. (2001) Neurology of ciguatera. *J. Neurol. Neurosurg. Psychiatry.* 70, 4-8.
- (5) Yasumoto, T. (2001) The chemistry and biological function of natural marine toxins. *Chem. Rec.* 1, 228-242.
- (6) Murata, M., Sasaki, M., Yokoyama, A., Iwashita, T., Gusovsky, F., Daly, J. W., and Yasumoto, T. (1992) Partial structures and binding studies of maitotoxin, the most potent marine toxin. *Bull. Soc. Pathol. Exot.* 85, 470-473.
- (7) Lombet, A., Bidard, J. N., and Lazdunski, M. (1987) Ciguatoxin and brevetoxins share a common receptor site on the neuronal voltage-dependent Na⁺ channel. *FEBS. Lett.* 219, 355-359.
- (8) Benoit, E., Juzans, P., Legrand, A. M., and Molgo, J. (1996) Nodal swelling produced by ciguatoxin-induced selective activation of sodium channels in myelinated nerve fibers. *Neuroscience* 71, 1121-1131.
- (9) Bidard, J. N., Vijverberg, H. P., Frelin, C., Chungue, E., Legrand, A. M., Bagnis, R., and Lazdunski, M. (1984) Ciguatoxin is a novel type of Na⁺ channel toxin. *J. Biol. Chem.* 259, 8353-8357.
- (10) Catterall, W. A., Cestele, S., Yarov-Yarovoy, V., Yu, F. H., Konoki, K., and Scheuer, T. (2007) Voltage-gated ion channels and gating modifier toxins. *Toxicon* 49, 124-141.
- (11) Molgo, J., Shimahara, T., and Legrand, A. M. (1993) Ciguatoxin, extracted from poisonous morays eels, causes sodium-dependent calcium mobilization in NG108-15 neuroblastoma x glioma hybrid cells. *Neurosci. Lett.* 158, 147-150.
- (12) Huang, J. M., Wu, C. H., and Baden, D. G. (1984) Depolarizing action of a red-tide dinoflagellate brevetoxin on axonal membranes. *J. Pharmacol. Exp. Ther.* 229, 615-621.

- (13) Murata, M., and Yasumoto, T. (2000) The structure elucidation and biological activities of high molecular weight algal toxins: maitotoxin, prymnesins and zooxanthellatoxins. *Nat. Prod. Rep.* 17, 293-314.
- (14) Nicolaou, K. C., and Frederick, M. O. (2007) On the structure of maitotoxin. *Angew. Chem. Int. Ed. Engl.* 46, 5278-5282.
- (15) Gusovsky, F., and Daly, J. W. (1990) Maitotoxin: a unique pharmacological tool for research on calcium-dependent mechanisms. *Biochem. Pharmacol.* 39, 1633-1639.
- (16) Lu, X. Z., Deckey, R., Jiao, G. L., Ren, H. F., and Li, M. (2013) Caribbean maitotoxin elevates $[Ca^{2+}]_i$ and activates non-selective cation channels in HIT-T15 cells. *World. J. Diabetes* 4, 70-75.
- (17) Sladeczek, F., Schmidt, B. H., Alonso, R., Vian, L., Tep, A., Yasumoto, T., Cory, R. N., and Bockaert, J. (1988) New insights into maitotoxin action. *Eur. J. Biochem.* 174, 663-670.
- (18) Ueda, H., Tamura, S., Harada, H., Yasumoto, T., and Takagi, H. (1986) The maitotoxin-evoked Ca^{2+} entry into synaptosomes is enhanced by cholera toxin. *Neurosci. Lett.* 67, 141-146.
- (19) Vale, C., Alfonso, A., Sunol, C., Vieytes, M. R., and Botana, L. M. (2006) Modulation of calcium entry and glutamate release in cultured cerebellar granule cells by palytoxin. *J. Neurosci. Res.* 83, 1393-1406.
- (20) Vale-Gonzalez, C., Gomez-Limia, B., Vieytes, M. R., and Botana, L. M. (2007) Effects of the marine phycotoxin palytoxin on neuronal pH in primary cultures of cerebellar granule cells. *J. Neurosci. Res.* 85, 90-98.
- (21) Wang, Y., Weiss, M. T., Yin, J., Frew, R., Tenn, C., Nelson, P. P., Vair, C., and Sawyer, T. W. (2009) Role of the sodium hydrogen exchanger in maitotoxin-induced cell death in cultured rat cortical neurons. *Toxicol.* 54, 95-102.
- (22) Reyes, J. G., Osses, N., Knox, M., Darszon, A., and Trevino, C. L. (2010) Glucose and lactate regulate maitotoxin-activated Ca^{2+} entry in spermatogenic cells: the role of intracellular $[Ca^{2+}]_i$. *FEBS. Lett.* 584, 3111-3115.
- (23) Meunier, F. A., Mattei, C., and Molgo, J. (2009) Marine toxins potently affecting neurotransmitter release. *Prog. Mol. Subcell. Biol.* 46, 159-186.
- (24) Martin, V., Vale, C., Bondu, S., Thomas, O. P., Vieytes, M. R., and Botana, L. M. (2013) Differential effects of crambescins and crambescidin 816 in voltage-gated sodium, potassium and calcium channels in neurons. *Chem. Res. Toxicol.* 26, 169-178.
- (25) Vale, C., Nicolaou, K. C., Frederick, M. O., Gomez-Limia, B., Alfonso, A., Vieytes, M. R., and Botana, L. M. (2007) Effects of azaspiracid-1, a potent cytotoxic agent, on primary neuronal cultures. A structure-activity relationship study. *J. Med. Chem.* 50, 356-363.
- (26) Hirama, M. (2005) Total synthesis of ciguatoxin CTX3C: a venture into the problems of ciguatera seafood poisoning. *Chem. Rec.* 5, 240-250.
- (27) Hirama, M., Oishi, T., Uehara, H., Inoue, M., Maruyama, M., Oguri, H., and Satake, M. (2001) Total synthesis of ciguatoxin CTX3C. *Science*, 294, 1904-1907.
- (28) Pedretti, A., Villa, L., and Vistoli, G. (2003) Atom-type description language: a universal language to recognize atom types implemented in the VEGA program. *Theoretical Chemistry Accounts* 109, 229-232.
- (29) Kita, M., and Uemura, D. (2010) Marine huge molecules: the longest carbon chains in natural products. *Chem. Rec.* 10, 48-52.

- (30) Yamaoka, K., Inoue, M., Miyahara, H., Miyazaki, K., and Hirama, M. (2004) A quantitative and comparative study of the effects of a synthetic ciguatoxin CTX3C on the kinetic properties of voltage-dependent sodium channels. *Br. J. Pharmacol.* 142, 879-889.
- (31) Ghiaroni, V., Fuwa, H., Inoue, M., Sasaki, M., Miyazaki, K., Hirama, M., Yasumoto, T., Rossini, G. P., Scalera, G., and Bigiani, A. (2006) Effect of ciguatoxin 3C on voltage-gated Na⁺ and K⁺ currents in mouse taste cells. *Chem. Senses* 31, 673-680.
- (32) Ghiaroni, V., Sasaki, M., Fuwa, H., Rossini, G. P., Scalera, G., Yasumoto, T., Pietra, P., and Bigiani, A. (2005) Inhibition of voltage-gated potassium currents by gambierol in mouse taste cells. *Toxicol. Sci.* 85, 657-665.
- (33) Freedman, S. B., Miller, R. J., Miller, D. M., and Tindall, D. R. (1984) Interactions of maitotoxin with voltage-sensitive calcium channels in cultured neuronal cells. *Proc. Natl. Acad. Sci. USA.* 81, 4582-4585.
- (34) Budde, T., Meuth, S., and Pape, H. C. (2002) Calcium-dependent inactivation of neuronal calcium channels. *Nat. Rev. Neurosci.* 3, 873-883.
- (35) Dechraoui, M. Y., Naar, J., Pauillac, S., and Legrand, A. M. (1999) Ciguatoxins and brevetoxins, neurotoxic polyether compounds active on sodium channels. *Toxicon* 37, 125-143.
- (36) Miller, R. J. (1991) The control of neuronal Ca²⁺ homeostasis. *Prog. Neurobiol.* 37, 255-285.
- (37) Berridge, M. J. (1997) Elementary and global aspects of calcium signalling. *J. Physiol.* 499 (Pt 2), 291-306.
- (38) Leist, M., and Nicotera, P. (1998) Calcium and neuronal death. *Rev. Physiol. Biochem. Pharmacol.* 132, 79-125.
- (39) Gutierrez, D., Diaz de Leon, L., and Vaca, L. (1997) Characterization of the maitotoxin-induced calcium influx pathway from human skin fibroblasts. *Cell Calcium* 22, 31-38.
- (40) Louzao, M. C., Vieytes, M. R., Yasumoto, T., Yotsu-Yamashita, M., and Botana, L. M. (2006) Changes in membrane potential: an early signal triggered by neurologically active phycotoxins. *Chem. Res. Toxicol.* 19, 788-793.
- (41) Meucci, O., Grimaldi, M., Scorziello, A., Govoni, S., Bergamaschi, S., Yasumoto, T., and Schettini, G. (1992) Maitotoxin-induced intracellular calcium rise in PC12 cells: involvement of dihydropyridine-sensitive and omega-conotoxin-sensitive calcium channels and phosphoinositide breakdown. *J. Neurochem.* 59, 679-688.
- (42) Kakizaki, A., Takahashi, M., Akagi, H., Tachikawa, E., Yamamoto, T., Taira, E., Yamakuni, T., and Ohizumi, Y. (2006) Ca²⁺ channel activating action of maitotoxin in cultured brainstem neurons. *Eur. J. Pharmacol.*, 536, 223-231.
- (43) Torreano, P. J., and Cohan, C. S. (2003) Calcium and voltage dependent inactivation of sodium and calcium currents limits calcium influx in *Helisoma* neurons. *J. Neurobiol.* 54, 439-456.
- (44) Perez, S., Vale, C., Alonso, E., Alfonso, C., Rodriguez, P., Otero, P., Alfonso, A., Vale, P., Hirama, M., Vieytes, M. R., and Botana, L. M. (2011) A comparative study of the effect of ciguatoxins on voltage-dependent Na⁺ and K⁺ channels in cerebellar neurons. *Chem. Res. Toxicol.* 24, 587-596.
- (45) Hidalgo, J., Liberona, J. L., Molgo, J., and Jaimovich, E. (2002) Pacific ciguatoxin-1b effect over Na⁺ and K⁺ currents, inositol 1,4,5-triphosphate content and intracellular Ca²⁺ signals in cultured rat myotubes. *Br. J. Pharmacol.* 137, 1055-1062.

- (46) Birinyi-Strachan, L. C., Gunning, S. J., Lewis, R. J., and Nicholson, G. M. (2005) Block of voltage-gated potassium channels by Pacific ciguatoxin-1 contributes to increased neuronal excitability in rat sensory neurons. *Toxicol. Appl. Pharmacol.* 204, 175-186.
- (47) Molgo, J., Comella, J. X., Shimahara, T., and Legrand, A. M. (1991) Tetrodotoxin-sensitive ciguatoxin effects on quantal release, synaptic vesicle depletion, and calcium mobilization. *Ann. N.Y. Acad. Sci.* 635, 485-488.
- (48) Satoh, E., Ishii, T., and Nishimura, M. (2001) The mechanism of maitotoxin-induced elevation of the cytosolic free calcium level in rat cerebrocortical synaptosomes. *Jpn. J. Pharmacol.* 85, 98-100.
- (49) Escobar, L. I., Salvador, C., Martinez, M., and Vaca, L. (1998) Maitotoxin, a cationic channel activator. *Neurobiology (Bp)* 6, 59-74.
- (50) Young, R. C., McLaren, M., and Ramsdell, J. S. (1995) Maitotoxin increases voltage independent chloride and sodium currents in GH4C1 rat pituitary cells. *Nat. Toxins.* 3, 419-427.
- (51) Soergel, D. G., Yasumoto, T., Daly, J. W., and Gusovsky, F. (1992) Maitotoxin effects are blocked by SK&F 96365, an inhibitor of receptor-mediated calcium entry. *Mol. Pharmacol.* 41, 487-493.
- (52) Musgrave, I. F., Seifert, R., and Schultz, G. (1994) Maitotoxin activates cation channels distinct from the receptor-activated non-selective cation channels of HL-60 cells. *Biochem. J.* 301 (Pt 2), 437-441.
- (53) Frew, R., Wang, Y., Weiss, T. M., Nelson, P., and Sawyer, T. W. (2008) Attenuation of maitotoxin-induced cytotoxicity in rat aortic smooth muscle cells by inhibitors of Na⁺/Ca²⁺ exchange, and calpain activation. *Toxicon* 51, 1400-1408.
- (54) Shono, Y., Kamouchi, M., Kitazono, T., Kuroda, J., Nakamura, K., Hagiwara, N., Ooboshi, H., Ibayashi, S., and Iida, M. (2010) Change in intracellular pH causes the toxic Ca²⁺ entry via NCX1 in neuron- and glia-derived cells. *Cell. Mol. Neurobiol.* 30, 453-460.
- (55) Mahnensmith, R. L., and Aronson, P. S. (1985) The plasma membrane sodium-hydrogen exchanger and its role in physiological and pathophysiological processes. *Circ. Res.* 56, 773-788.
- (56) Vale, C., Gomez-Limia, B., Vieytes, M. R., and Botana, L. M. (2007) Mitogen-activated protein kinases regulate palytoxin-induced calcium influx and cytotoxicity in cultured neurons. *Br. J. Pharmacol.* 152, 256-266.

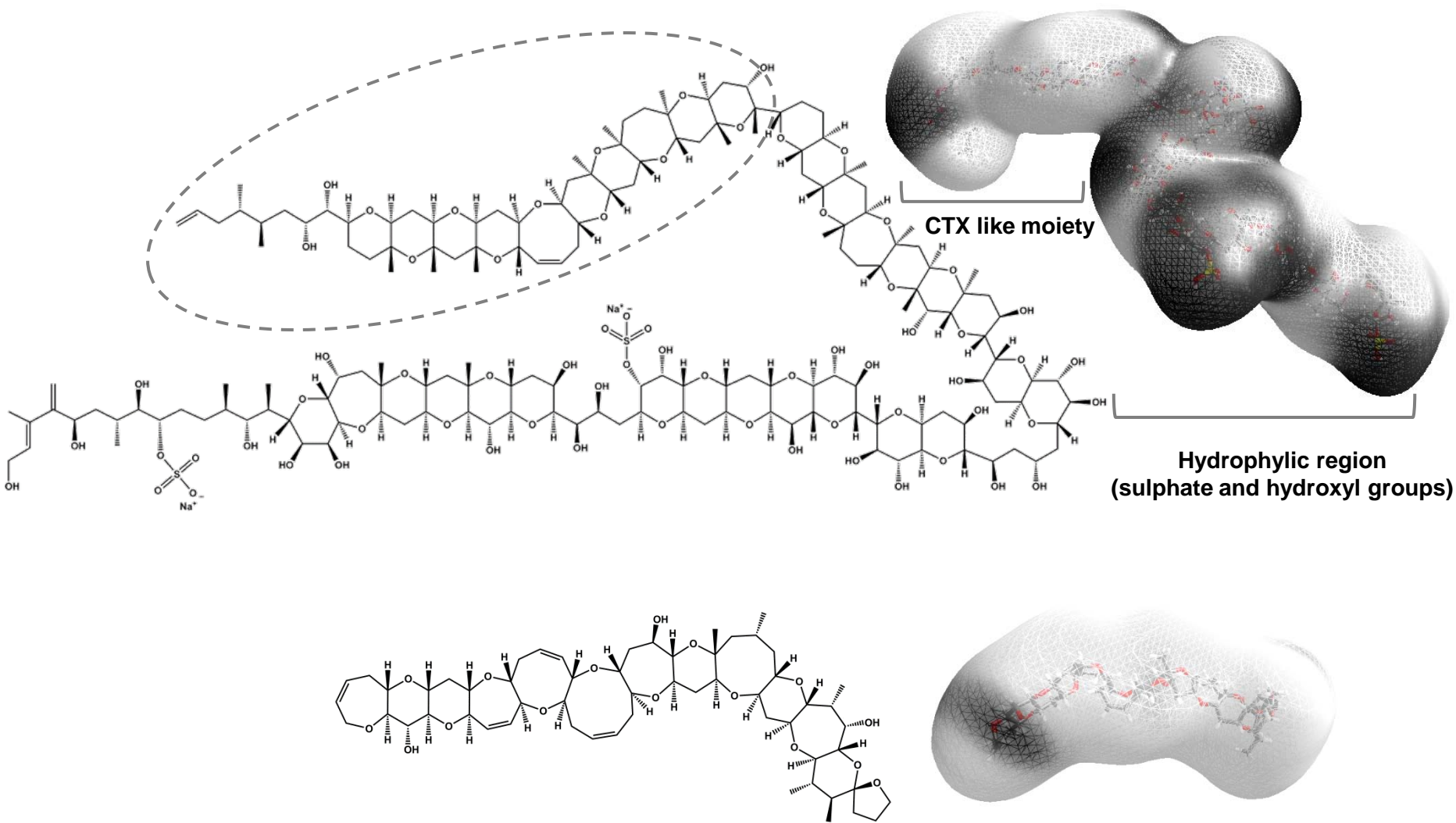


Figure 1

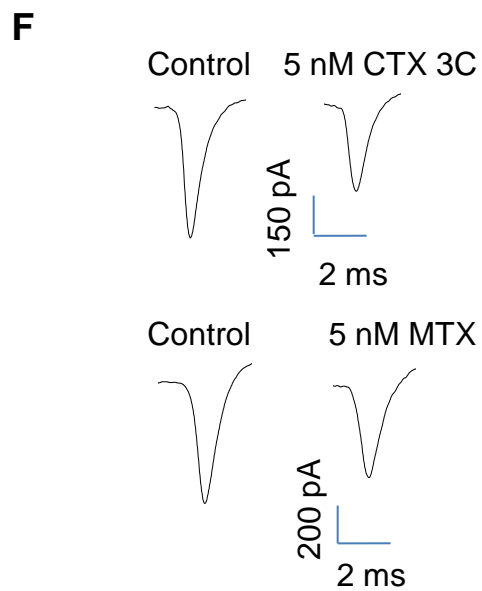
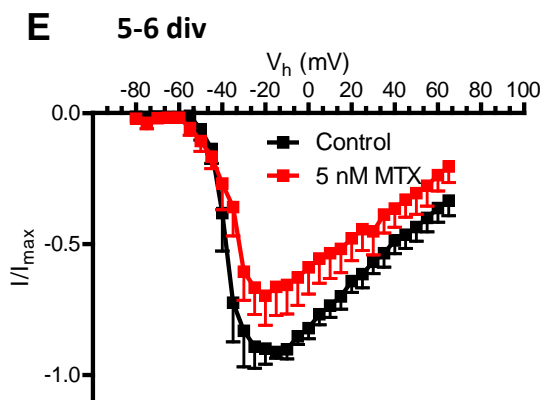
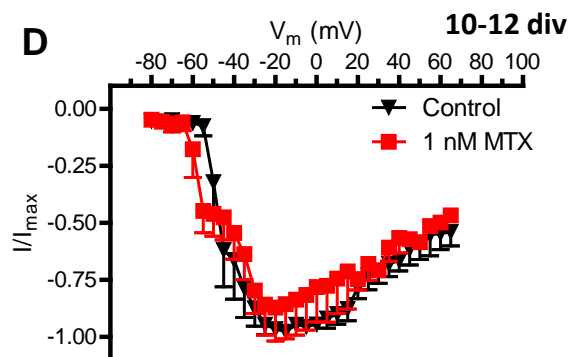
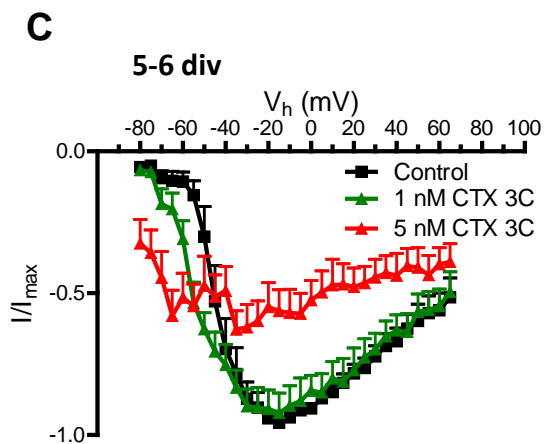
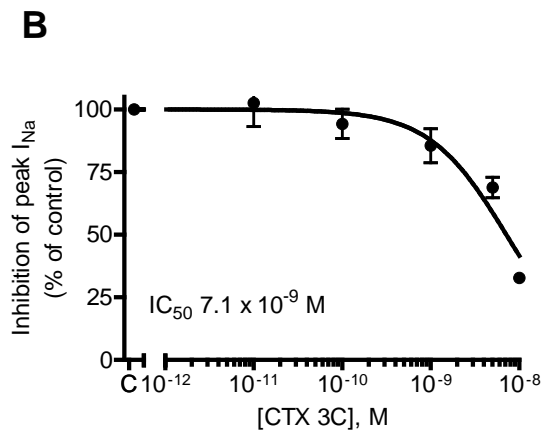
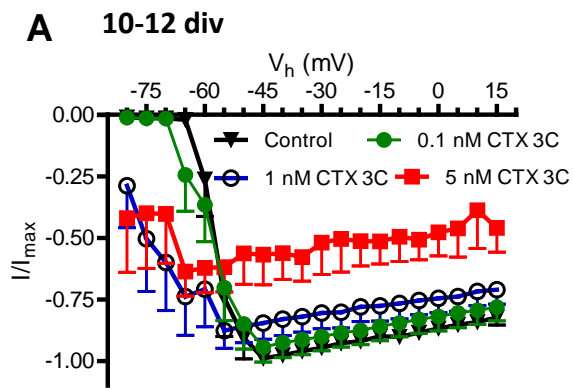


Figure 2

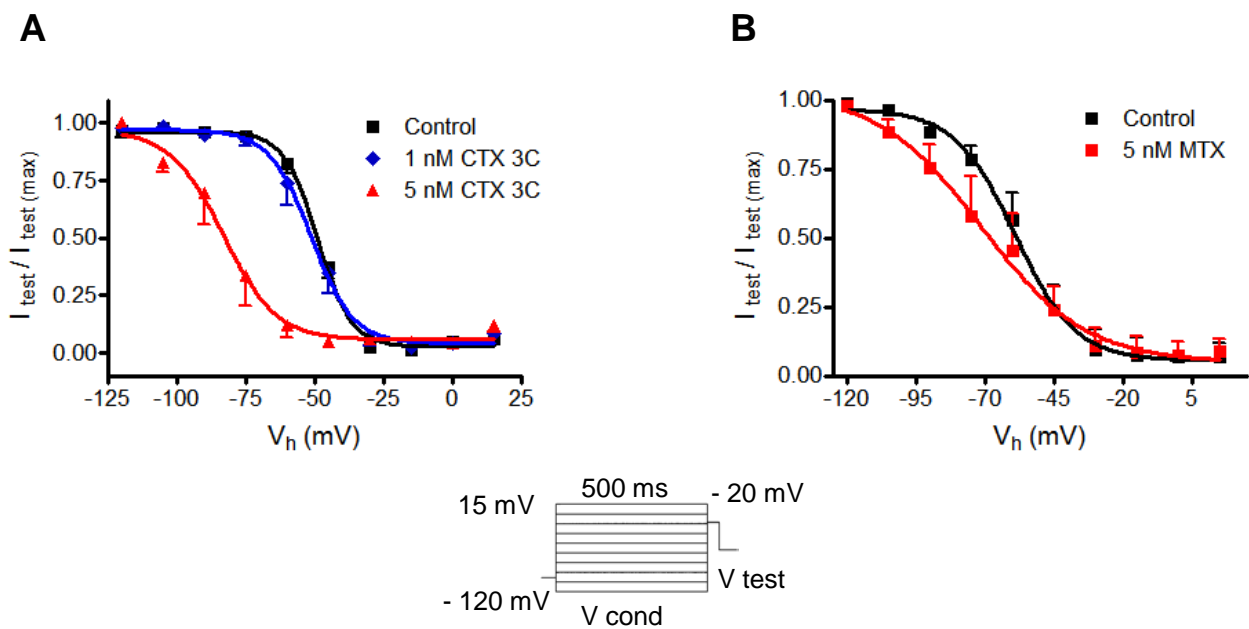


Figure 3

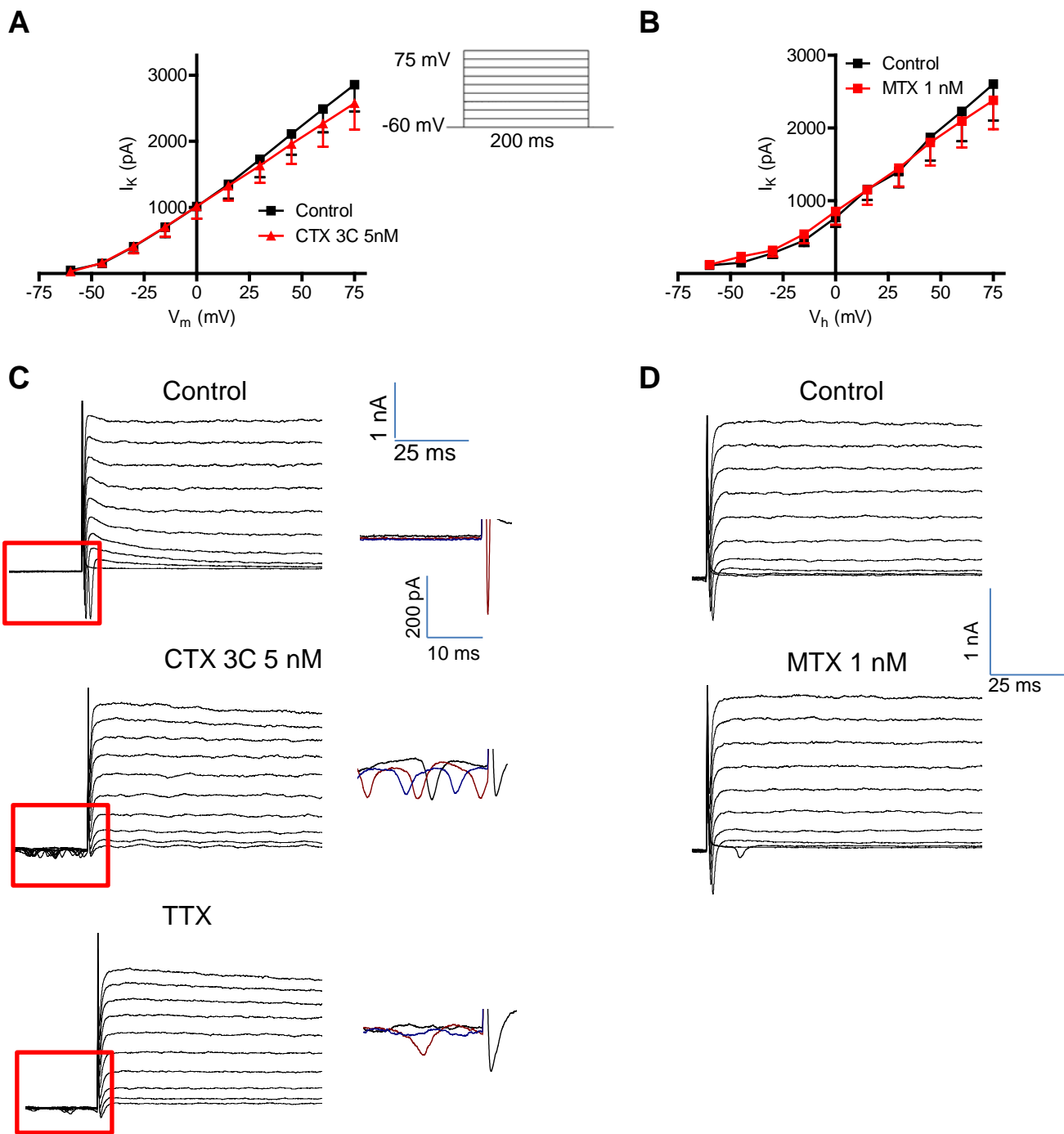


Figure 4

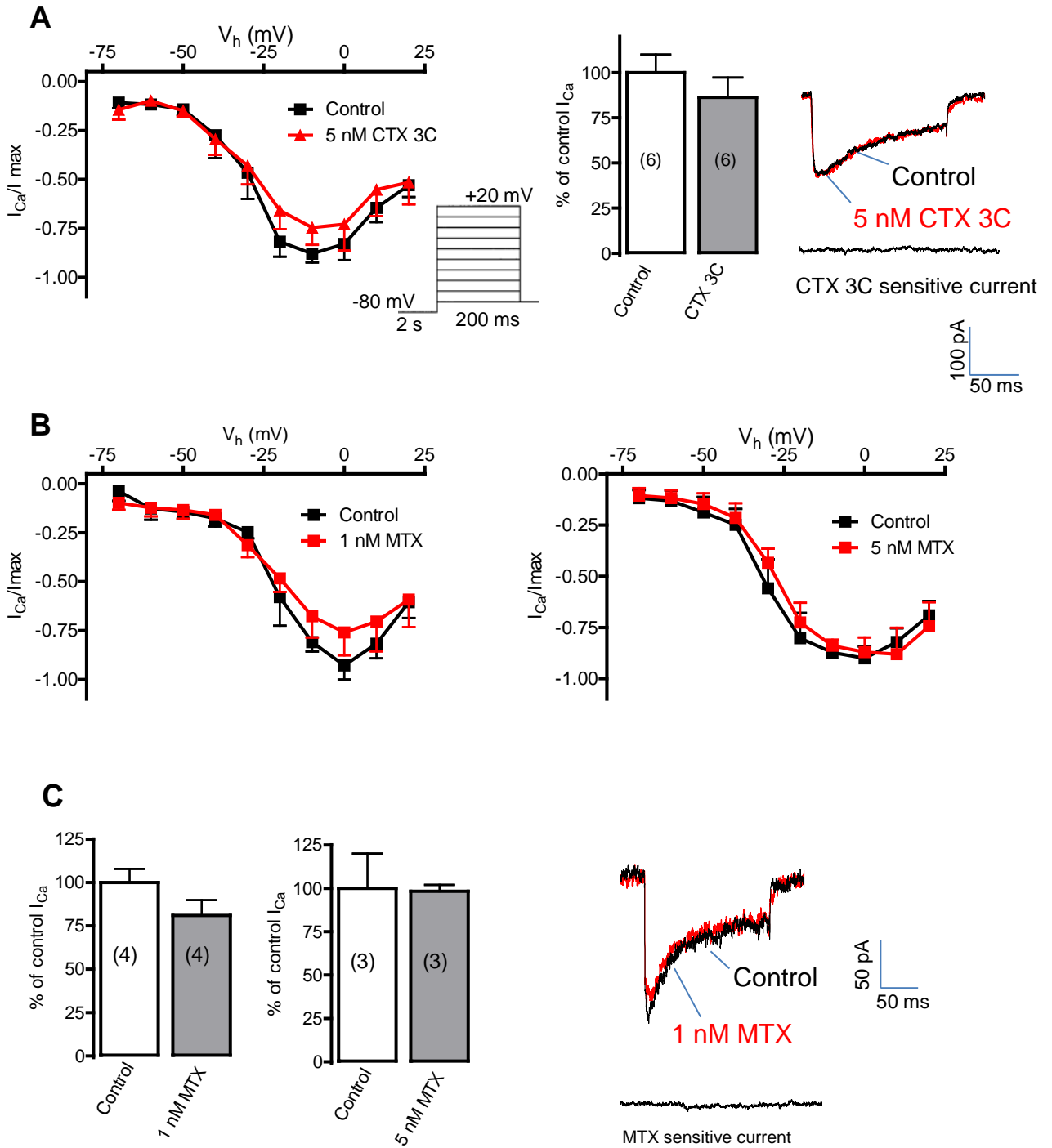


Figure 5

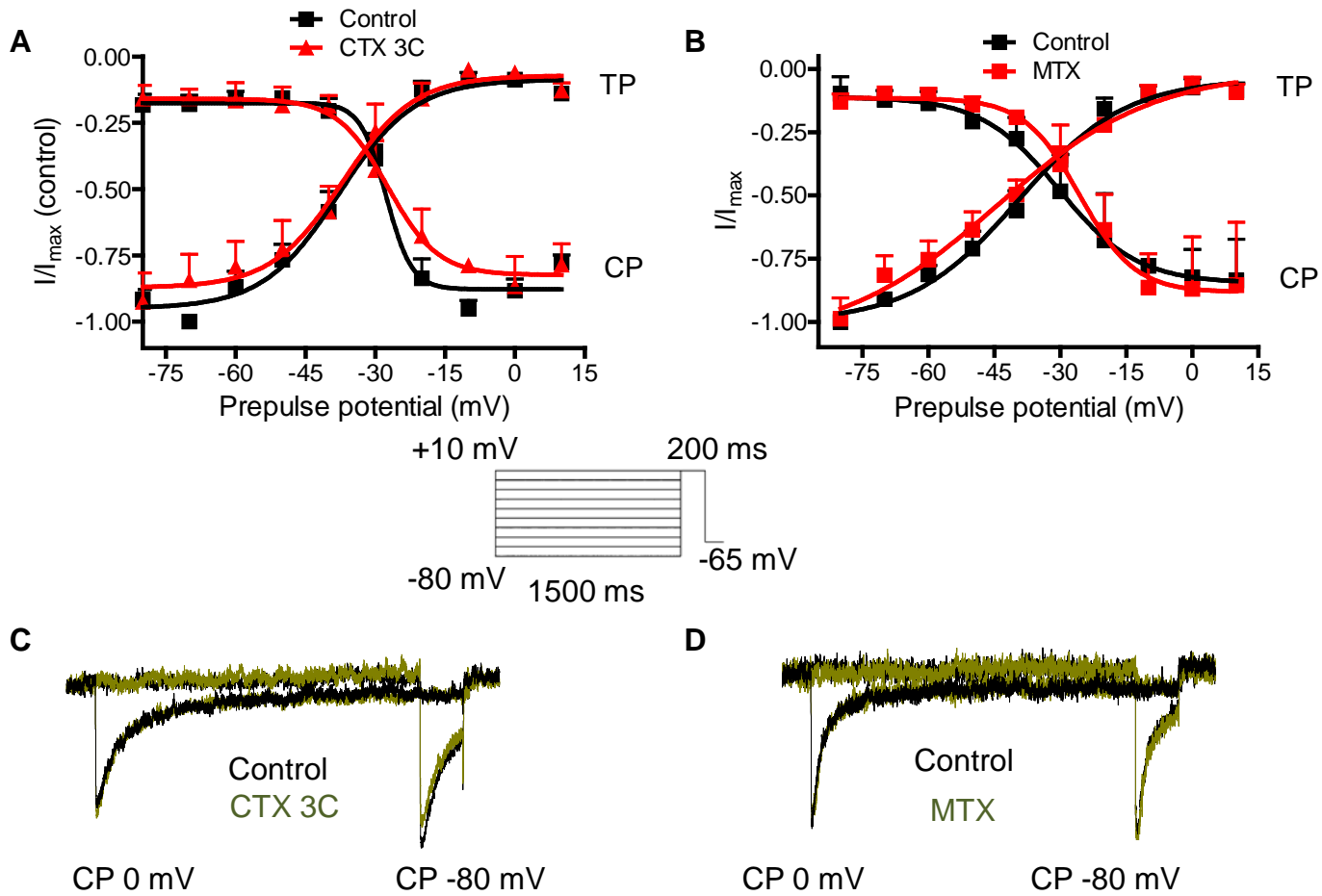


Figure 6

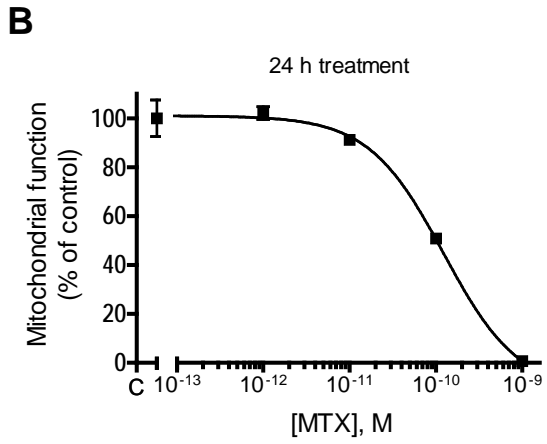
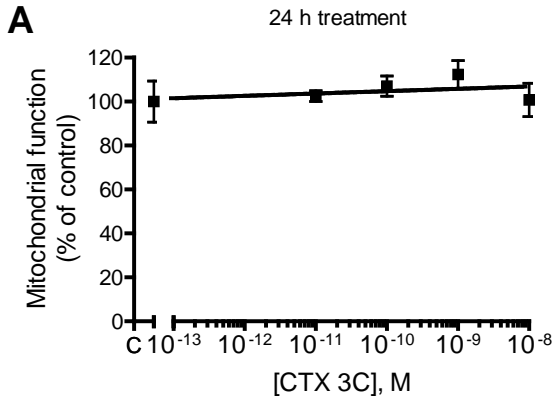


Figure 7

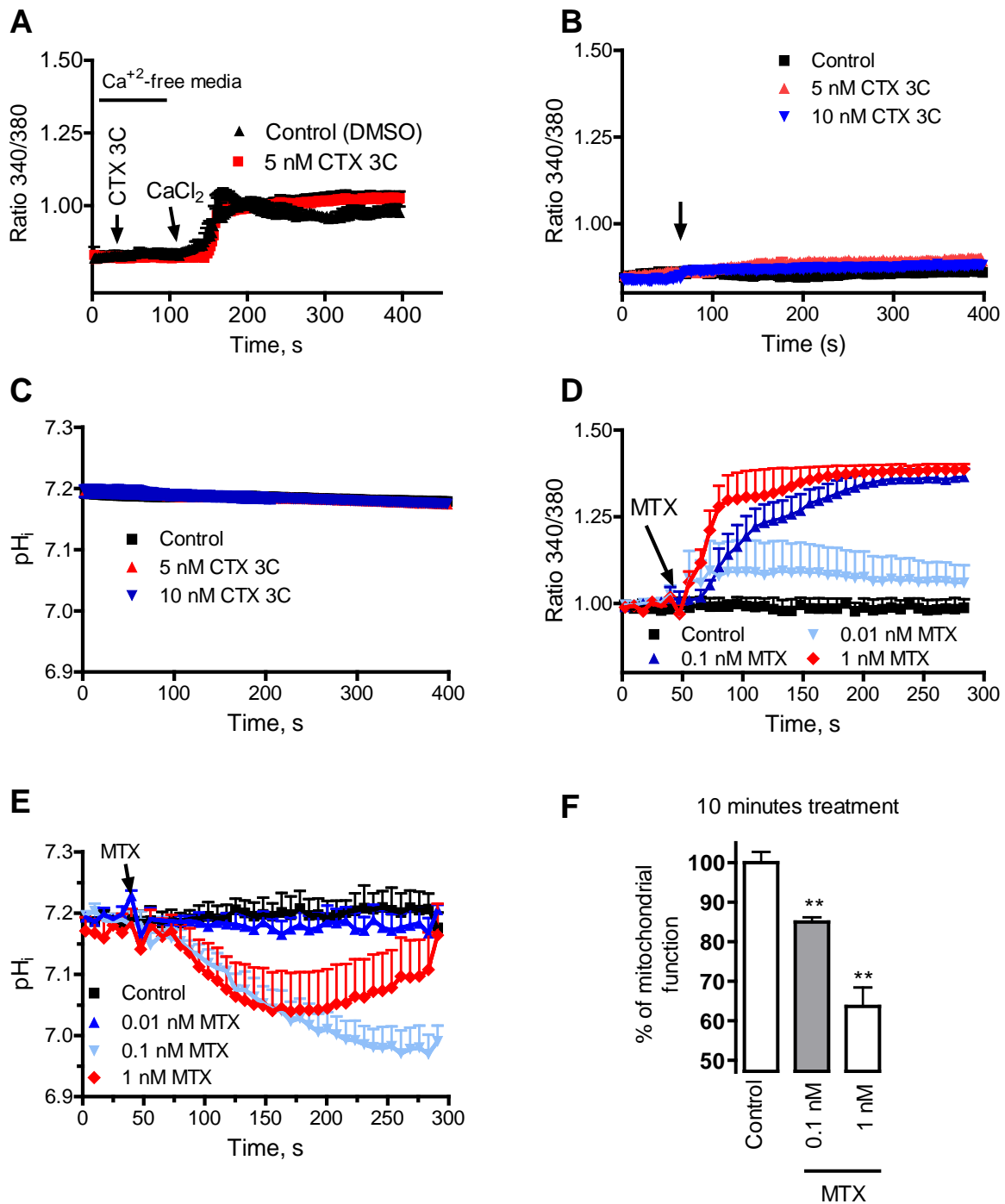


Figure 8

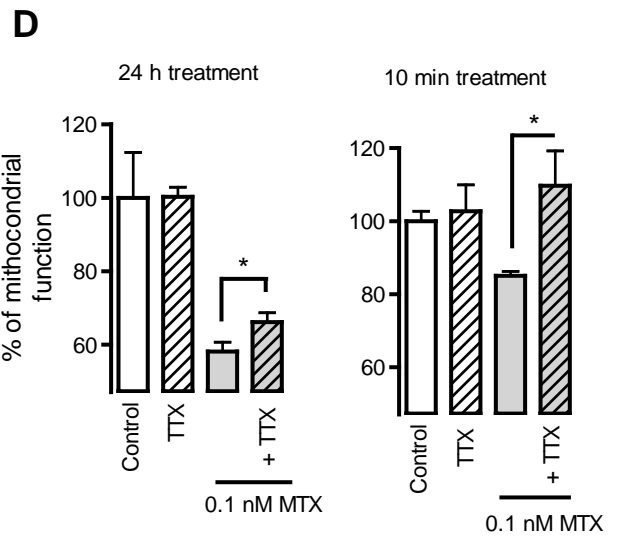
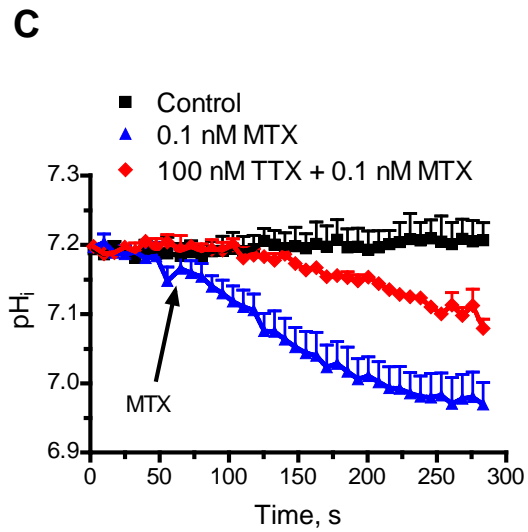
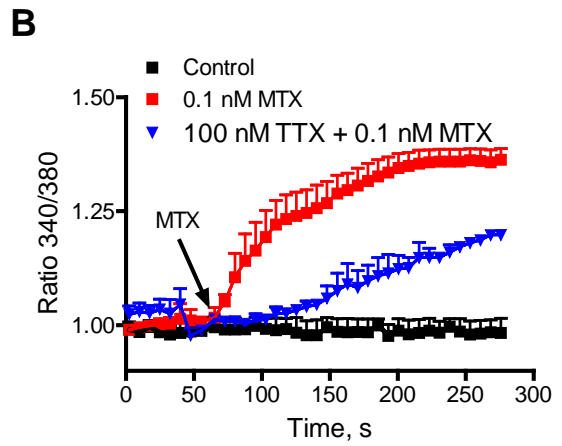
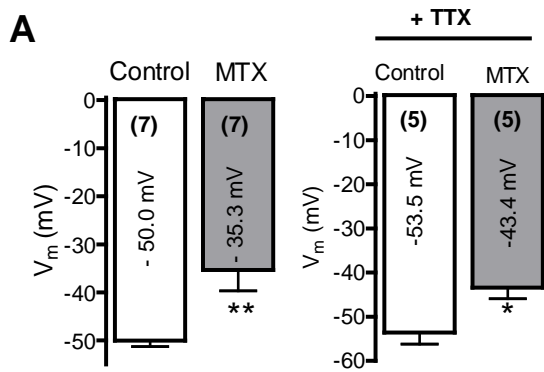
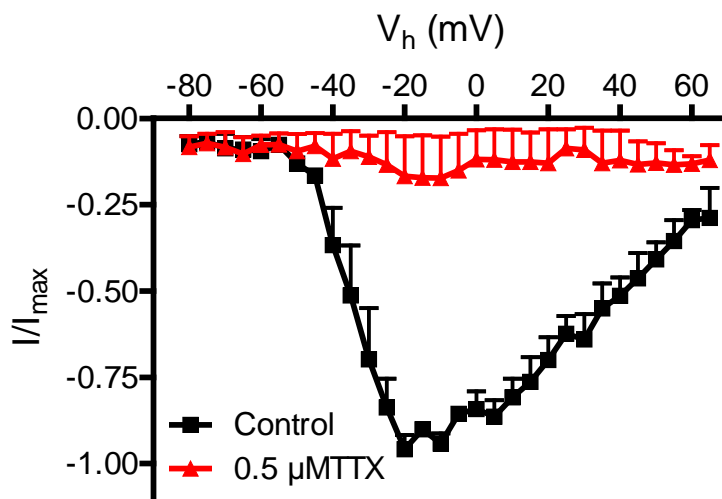


Figure 9



Supplementary Figure 1. Voltage-gated sodium currents of cortical neurons are tetrodotoxin-sensitive. I-V curves showing normalized sodium currents amplitudes in the absence and in presence of 0.5 μ M TTX in the extracellular solution.